

Flood Volcanism in the Northern High Latitudes of Mercury Revealed by MESSENGER

James W. Head,^{1*} Clark R. Chapman,² Robert G. Strom,³ Caleb I. Fassett,¹ Brett W. Denevi,⁴ David T. Blewett,⁴ Carolyn M. ErNST,⁴ Thomas R. Watters,⁵ Sean C. Solomon,⁶ Scott L. Murchie,⁴ Louise M. Prockter,⁴ Nancy L. Chabot,⁴ Jeffrey J. Gillis-Davis,⁷ Jennifer L. Whitten,¹ Timothy A. Goudge,¹ David M. H. Baker,¹ Debra M. Hurwitz,¹ Lillian R. Ostrach,⁸ Zhiyong Xiao,^{3,9} William J. Merline,² Laura Kerber,¹ James L. Dickson,¹ Jürgen Oberst,¹⁰ Paul K. Byrne,⁶ Christian Klimczak,⁶ Larry R. Nittler⁶

MESSENGER observations from Mercury orbit reveal that a large contiguous expanse of smooth plains covers much of Mercury's high northern latitudes and occupies more than 6% of the planet's surface area. These plains are smooth, embay other landforms, are distinct in color, show several flow features, and partially or completely bury impact craters, the sizes of which indicate plains thicknesses of more than 1 kilometer and multiple phases of emplacement. These characteristics, as well as associated features, interpreted to have formed by thermal erosion, indicate emplacement in a flood-basalt style, consistent with x-ray spectrometric data indicating surface compositions intermediate between those of basalts and komatiites. The plains formed after the Caloris impact basin, confirming that volcanism was a globally extensive process in Mercury's post-heavy bombardment era.

The Mariner 10 flybys of Mercury during 1974–1975 revealed that the planet had several large areas of smooth plains containing relatively fewer impact craters. Whether the Caloris basin-related plains were volcanic (1–3) or consisted of fluidized impact ejecta as seen on the Moon (4) was a matter of debate until the MESSENGER flybys in 2008–2009 confirmed their volcanic origin and that volcanism was widespread on Mercury (5–11). Uncertainties remaining after those flybys included the origin of other plains occurrences, the volcanic styles and modes of emplacement of volcanic plains (12), their global extent and elemental composition, and the time span of their emplacement (13). Here, we used high-resolution images provided by MESSENGER now in orbit around Mercury to address these issues.

Images from the Mariner 10 (2) and MESSENGER flybys (8, 9, 13) hinted that an area of smooth plains (14) and a large impact basin (2) were present at high northern latitudes, an association perhaps indicating an impact origin for these plains [e.g., (4, 14)].

MESSENGER observations during the first Mercury year in orbit show that these smooth plains are less heavily cratered than their surroundings (Fig. 1 and fig. S1) and form a contiguous unit extending around the pole covering $\sim 4.7 \times 10^6 \text{ km}^2$, or about 6% of the surface area of Mercury. Mercury Dual Imaging System

(MDIS) (15) color data indicate that these smooth plains are homogeneous, differ in color from the surrounding more heavily cratered terrain, and are comparable to high-reflectance plains mapped elsewhere on Mercury (8, 9).

Ghost craters (Fig. 1) (5, 7), preexisting impact craters that have been partially or completely buried and are now seen as relict rings of ridges in the overlying plains, can provide clues as to the thickness and mode of emplacement of younger deposits. Under the assumption that the crater was fresh at the time of burial, morphometric relations (depth/diameter ratio; rim crest height above adjacent terrain) (16) can be used to estimate the depth of burial and thus the thickness of the plains unit. We have mapped more than a dozen buried craters at least 60 to 70 km in diameter (Fig. 1) within the northern smooth plains. Ghost craters >100 km in diameter in the interior of the smooth plains indicate that plains thicknesses locally exceed 1 to 2 km. The density of smaller ghost craters varies across the smooth plains, which suggests that the plains unit thins toward the areas hosting clusters of such features and that when the plains were emplaced, broad lows occupied those areas where small ghost craters are absent. If these lows mark one or more degraded impact basins (2), the lack of clear circular basin outlines indicates that any such basins would be highly degraded and therefore comparable in age to some of the oldest terrain on Mercury (13). An alternative interpretation of the smaller ghost craters in the smooth plains interior

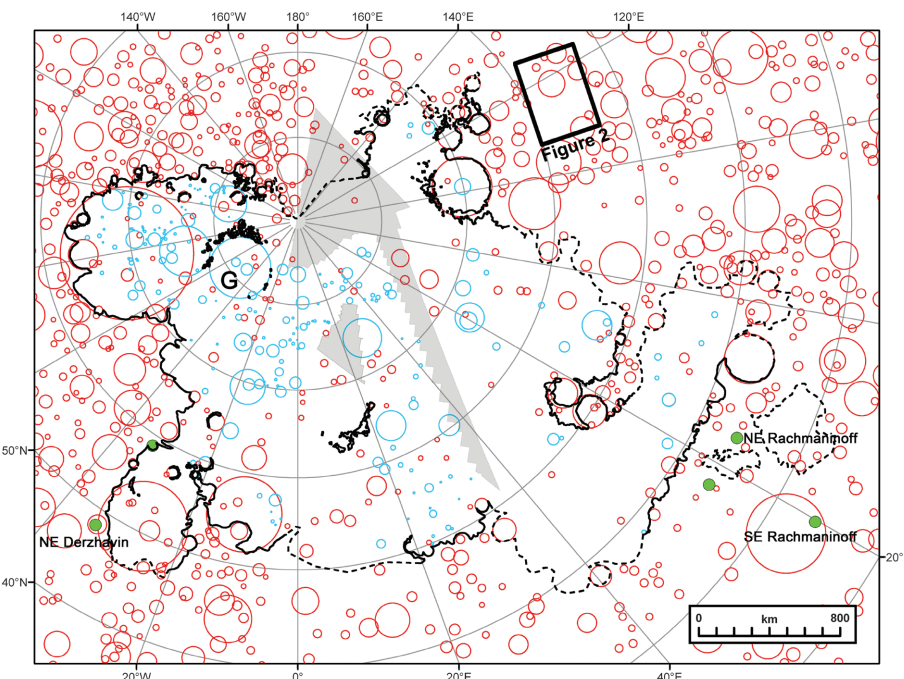
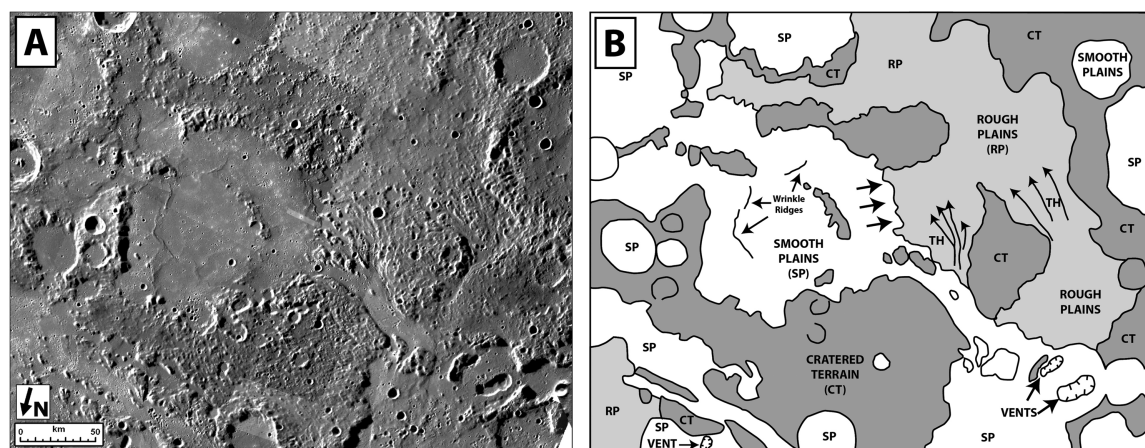


Fig. 1. Distribution of smooth plains and adjacent older units at high northern latitudes on Mercury. Smooth plains are outlined in black (solid, certain; dashed, approximate); impact craters >20 km in diameter are denoted by red circles (13), ghost craters within the plains by blue circles (the letter G denotes the Goethe basin), and pits and pyroclastic deposits by green dots [including named features (6) and others newly recognized]. Gray areas denote gaps in MDIS imaging coverage as of this writing. Major trends of wrinkle ridges in the region are given in fig. S1.

*To whom correspondence should be addressed. E-mail: james_head@brown.edu

Fig. 2. Image (A) and sketch map (B) of the assemblage of volcanic flow-related features shown in Fig. 3, A to C; blunt arrows, flow front-like embayment (see Fig. 3C); long arrows, teardrop-shaped hills (TH). Image location (see also Fig. 1) and MESSENGER image numbers are given in the supporting online material (SOM).



is that initial phases of flooding buried older craters, but new craters formed before subsequent stages of flooding. Overall, the northern smooth plains (Fig. 1) have a distribution similar to that of some large irregular maria such as Oceanus Procellarum (12), further evidence that they are not associated with a relatively young impact basin. The plains contain wrinkle ridges and broader arches that appear to postdate the surface of the smooth plains and trend across them (fig. S1) in patterns different from those of the Caloris basin on Mercury (17) and circular mare-filled basins on the Moon (18). We found no evidence of a nearby impact basin (2) of an age comparable to that of the northern smooth plains (13) (Fig. 1) that might be consistent with the plains having an impact origin as ponded basin ejecta or impact melt sheets (4).

We performed a detailed search for evidence of volcanic source vents, edifices, or lava flow features (channels, sinuous rilles, flow fronts). Mariner 10 and the MDIS flyby image resolutions were not optimal for the type of characterization that could lead to confident identification of volcanic emplacement style (19), although volcanic pit craters, a low shield, and plains of volcanic origin (5–9) were documented in flyby data. Although MDIS orbital image resolution is sufficient to resolve a wide range of volcanic edifices (19), none were identified within the northern plains (Fig. 1). Many lunar mare basalts tend to collect in circular impact basins and irregularly shaped topographic lows, often obscuring volcanic source vents. It is also possible that any such features would be buried by thick lavas characterized by high effusion rates, large volumes, and often low viscosity, as seen in flood basalts and komatiites on Earth (20–24).

Examination of areas marginal to large featureless volcanic provinces often provides clues to their modes of emplacement (20, 21). Adjacent to the northern smooth plains (Fig. 1, Fig. 2, and fig. S1) is an unusual assemblage of pits 5 to 10 km in diameter (Fig. 3A), teardrop-shaped hills similar to water-carved outflow channel-related terrain on Mars (25) (Fig. 3B), rough plains, and distal lobate-margined smooth plains (Fig. 3C).

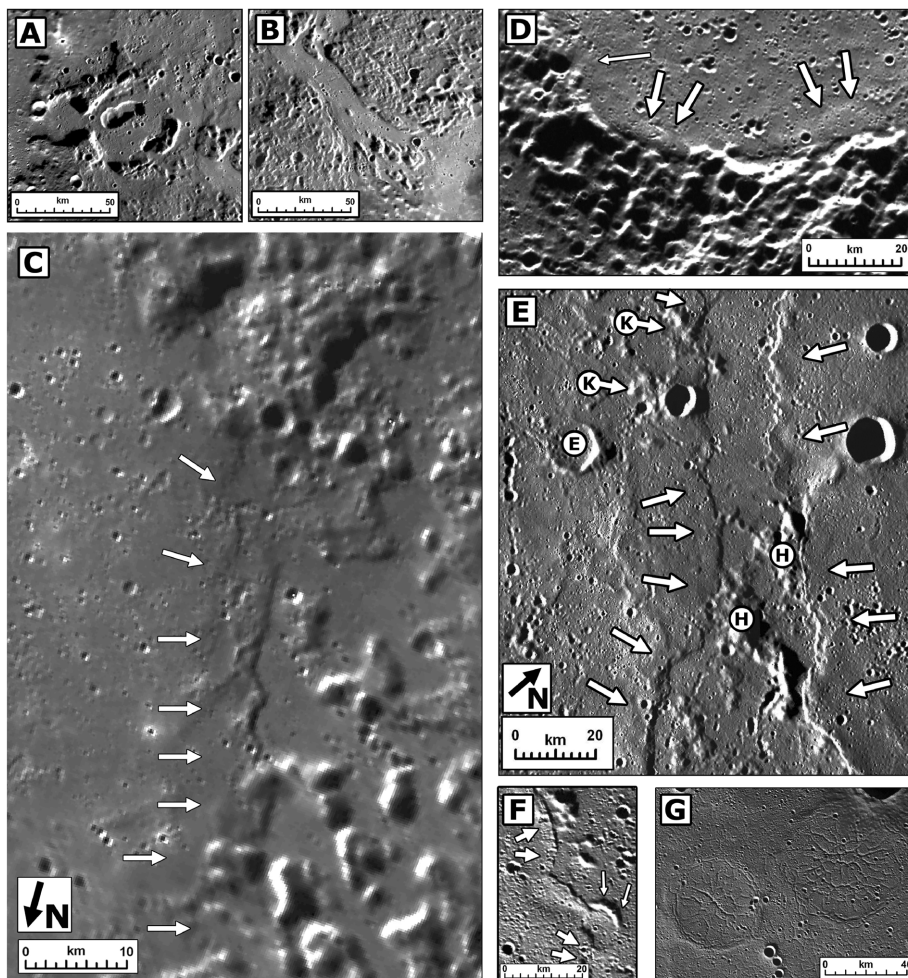


Fig. 3. Features interpreted to be related to lava flows in the northern smooth plains and vicinity. (A) Pits interpreted as source vents. (B) Teardrop-shaped hills and channel. (C) Distal smooth plains (left) embaying rough plains (right) (see Fig. 2) along a flow front-like contact (arrows). (D) Steep flow margin (broad arrows) within a flooded impact crater; narrow arrow points to possible flooding of a smaller crater. (E) Candidate lava flow fronts (arrows) embaying crater (E) and flooding the hills (H) between flow fronts to form kipukas (K). (F) Evidence for a flow front (broad arrows) descending into a preexisting crater (narrow arrows; note adjacent depressed part of flow). (G) Fissures inside flooded craters in the Goethe basin (G in Fig. 1). The location of these images and MESSENGER image numbers are given in the SOM.

We interpret the pits to be source vents and the teardrop-shaped hills to be regions where lava has sculpted underlying terrain, on the grounds

that aqueous erosion is precluded by Mercury's surface environment (26). These features are consistent with the rapid emplacement of high-

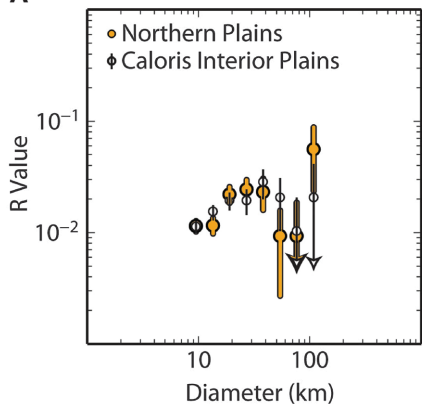
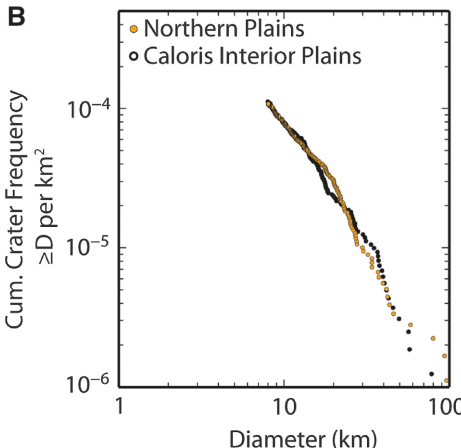
A**B**

Fig. 4. Size-frequency distribution of impact craters >8 km in diameter superposed on the northern smooth plains compared with those on the plains inside the Caloris basin: (A) R plot, (B) cumulative plot. Both plots show that the distributions for the two plains areas are statistically indistinguishable, and thus the two units are the same age to within statistical error. Areas measured, crater locations, and explanation of plots are given in the SOM.

temperature, low-viscosity flood lavas and the thermal erosion of subjacent terrain as seen on the Moon (12) and in connection with komatiitic lavas on Earth (23, 24). A broad channel filled with smooth plains (Fig. 3B) extends more than 150 km from the vicinity of the vents, filling a degraded crater ~ 115 km in diameter (Fig. 2 and Fig. 3C) and showing a flow front-like scarp contact with the teardrop-shaped hill terrain (Fig. 3C). Although morphologically similar to some contractional tectonic wrinkle ridges and lobate scarps (17), the scarp marks the edge of where the smooth unit embays and covers the sculpted terrain, indicating a flow contact. This contact relationship provides clues to the nature of flow fronts in the contiguous northern smooth plains.

The least ambiguous flow front margins are those that embay degraded crater rims. MDIS images show a steep flow margin, a broad rim crest (Fig. 3D, large arrows), and a depressed area interior to the flow front (27)—features typical of inflated flood lavas (28) or flows that have drained or undergone cooling and solidification. Flow fronts within the smooth plains themselves are difficult to locate with confidence because wrinkle ridges, tectonic features that can mimic flow front morphologies (12, 17, 18, 27), are abundant, but numerous examples of candidate flow fronts exist (Fig. 3, E and F).

The crenulated nature of parts of the smooth plains (Fig. 3, C, E, and F; see arrows) are interpreted to represent a similar series of flow fronts in the interior of the continuous northern smooth plains (compare to Fig. 2 and Fig. 3C). At one location (Fig. 3E, broad arrows) the sharp edges of two units face each other across a broad low. The western unit appears to embay an older crater, and kipukas of rough hills are preserved in the adjacent low between the units. The eastern unit also abuts and partly embays the hills. At another location (Fig. 3F, broad arrows), a flow partially embays

and descends into a preexisting ~ 10 -km-diameter crater (narrow arrows), creating a depressed area in the flow itself, a behavior typical of flood lavas (20). In addition, several ghost rings of buried craters show an unusual network of fractures (Fig. 3G), possibly the product of some combination of subsurface flow drainage, cooling, vertical motions, and larger-scale deformation; if related to extensive lava flooding, their large size (40 to 45 km) suggests flood lava-like volumes (20).

In summary, the orbital MDIS data reveal multiple lines of evidence that support the interpretation that the northern smooth plains were emplaced in a flood lava mode. Moreover, evidence for flow fronts extending over tens to hundreds of kilometers (Fig. 2 and Fig. 3, C and E) and lava-related erosion of the substrate suggest high effusion rates (12, 27) and possibly high-temperature, low-viscosity lavas (20–24, 27). Indeed, MESSENGER X-Ray Spectrometer (XRS) data (29) indicate that Mercury's average surface composition differs from that of the other terrestrial planets. In particular, Mg/Si, Al/Si, and Ca/Si ratios lie between those typical of basalt and more ultramafic rocks comparable to terrestrial komatiites, which are high-Mg (22), high-temperature, low-viscosity lavas (23) that erupted mostly during the Archean on Earth. More complete XRS coverage during the orbital mission will allow the compositions of individual occurrences of plains to be distinguished.

The size-frequency distribution of impact craters >8 km in diameter superposed on the plains (Fig. 4 and figs. S1 and S2) shows that the northern plains are comparable in age to the smooth plains that fill and surround the Caloris basin (11, 13, 30). Thus, this extensive occurrence of northern high-latitude smooth plains is Calorian (2) in age, dating from near the end of late heavy bombardment ~ 3.7 to 3.8 billion years ago (11). Unlike the plains associated with the Caloris

basin, however, the northern plains are unrelated to one or more young impact basins, indicating that large-volume eruptions of lavas on Mercury occurred independent of the largest cratering events. No regional variations in crater size-frequency distribution across the northern plains have been detected. This result, together with the indication from MDIS color images that reflectance and color are essentially homogeneous across the entire plains, supports the hypothesis that the northern smooth plains differ in character and composition from the series of mineralogically distinctive basalts emplaced over an extended period of time in most mare regions on the Moon (31). On the basis of a combination of geological and geochemical (29) observations, we conclude that the period near the end of late heavy bombardment on Mercury was characterized by extensive partial melting of the mantle and the widespread eruption of flood lavas with high effusion rates.

References and Notes

1. B. C. Murray, R. G. Strom, N. J. Trask, D. E. Gault, *J. Geophys. Res.* **80**, 2508 (1975).
2. P. D. Spudis, J. E. Guest, in *Mercury*, F. Vilas, C. R. Chapman, M. S. Matthews, Eds. (Univ. of Arizona Press, Tucson, AZ, 1988), pp. 118–164.
3. M. S. Robinson, P. G. Lucey, *Science* **275**, 197 (1997).
4. D. E. Wilhelms, *Icarus* **28**, 551 (1976).
5. J. W. Head et al., *Science* **321**, 69 (2008).
6. L. Kerber et al., *Planet. Space Sci.* 10.1016/j.pss.2011.03.020 (2011).
7. J. W. Head et al., *Earth Planet. Sci. Lett.* **285**, 227 (2009).
8. M. S. Robinson et al., *Science* **321**, 66 (2008).
9. B. W. Denewi et al., *Science* **324**, 613 (2009).
10. S. L. Murchie et al., *Science* **321**, 73 (2008).
11. R. G. Strom et al., *Planet. Space Sci.* 10.1016/j.pss.2011.03.018 (2011).
12. J. W. Head III, L. Wilson, *Geochim. Cosmochim. Acta* **56**, 2155 (1992).
13. C. I. Fassett, S. J. Kadish, J. W. Head, S. C. Solomon, R. G. Strom, *Geophys. Res. Lett.* **38**, L10202 (2011).
14. M. J. Gollier, J. M. Boyce, *Geologic Map of the Borealis Region (H-1) of Mercury* (Misc. Invest. Ser. I-1660, U.S. Geological Survey, Denver, CO, 1984).
15. S. E. Hawkins III et al., *Space Sci. Rev.* **131**, 247 (2007).
16. R. J. Pike, in *Mercury*, F. Vilas, C. R. Chapman, M. S. Matthews, Eds. (Univ. of Arizona Press, Tucson, AZ, 1988), pp. 165–273.
17. T. R. Watters et al., *Earth Planet. Sci. Lett.* **285**, 309 (2009).
18. D. E. Wilhelms, *The Geologic History of the Moon* (Prof. Pub. 1348, U.S. Geological Survey, Denver, CO, 1987).
19. S. M. Milkovich, J. W. Head, L. Wilson, *Meteorit. Planet. Sci.* **37**, 1209 (2002).
20. T. Thordarson, S. Self, *J. Geophys. Res.* **103**, (B11), 27411 (1998).
21. M. F. Coffin, O. Eldholm, *Geology* **21**, 515 (1993).
22. N. T. Arndt, *Komatiite* (Cambridge Univ. Press, Cambridge, 2008).
23. H. E. Huppert, R. S. J. Sparks, J. S. Turner, N. T. Arndt, *Nature* **309**, 19 (1984).
24. D. A. Williams, R. C. Kerr, C. M. Lesher, S. J. Barnes, *J. Volcanol. Geotherm. Res.* **110**, 27 (2001).
25. M. H. Carr, J. W. Head III, *Earth Planet. Sci. Lett.* **294**, 185 (2010).
26. D. M. Hunten, D. E. Shemansky, T. H. Morgan, in *Mercury*, F. Vilas, C. R. Chapman, M. S. Matthews, Eds. (Univ. of Arizona Press, Tucson, AZ, 1988), pp. 562–612.
27. L. Wilson, J. W. Head, *Geophys. Res. Lett.* **35**, L23205 (2008).

28. K. J. Hon, J. Kaauhikaua, R. Denlinger, K. Mackay, *Geol. Soc. Am. Bull.* **106**, 351 (1994).
29. L. R. Nittler *et al.*, *Science* **333**, 1847 (2011).
30. C. I. Fassett *et al.*, *Earth Planet. Sci. Lett.* **285**, 297 (2009).
31. H. Hiesinger, J. W. Head III, U. Wolf, R. Jaumann, G. Neukum, in *Recent Advances and Current Research Issues in Lunar Stratigraphy*, W. A. Ambrose,

D. A. Williams, Eds. (Special Paper 477, Geological Society of America, Boulder, CO, 2011), pp. 1–51.

Acknowledgments: We thank the MESSENGER team for development and flight operations. The NASA Discovery Program supports the MESSENGER mission through contract NAS5-97271 to The Johns Hopkins University Applied Physics Laboratory and NASW-00002 to the Carnegie Institution of Washington.

Supporting Online Material

www.sciencemag.org/cgi/content/full/333/6051/1853/DC1

SOM Text

Figs. S1 to S3

1 August 2011; accepted 5 September 2011
10.1126/science.1211997

Hollows on Mercury: MESSENGER Evidence for Geologically Recent Volatile-Related Activity

David T. Blewett,^{1,*} Nancy L. Chabot,¹ Brett W. Denevi,¹ Carolyn M. Ernst,¹ James W. Head,² Noam R. Izenberg,¹ Scott L. Murchie,¹ Sean C. Solomon,³ Larry R. Nittler,³ Timothy J. McCoy,⁴ Zhiyong Xiao,^{5,6} David M. H. Baker,² Caleb I. Fassett,² Sarah E. Braden,⁷ Jürgen Oberst,⁸ Frank Scholten,⁸ Frank Preusker,⁸ Debra M. Hurwitz²

High-resolution images of Mercury's surface from orbit reveal that many bright deposits within impact craters exhibit fresh-appearing, irregular, shallow, rimless depressions. The depressions, or hollows, range from tens of meters to a few kilometers across, and many have high-reflectance interiors and halos. The host rocks, which are associated with crater central peaks, peak rings, floors, and walls, are interpreted to have been excavated from depth by the crater-forming process. The most likely formation mechanisms for the hollows involve recent loss of volatiles through some combination of sublimation, space weathering, outgassing, or pyroclastic volcanism. These features support the inference that Mercury's interior contains higher abundances of volatile materials than predicted by most scenarios for the formation of the solar system's innermost planet.

The MESSENGER spacecraft entered orbit about Mercury on 18 March 2011, after which the Mercury Dual Imaging System (MDIS) (*1*) acquired high-spatial-resolution images. Many of the images reveal an unusual landform on Mercury, characterized by irregularly shaped, shallow, rimless depressions, commonly in clusters and in association with high-reflectance materials. Here, we describe this class of landform and its distribution and suggest that it indicates recent volatile-related activity.

MESSENGER is engaged in global imaging of Mercury's surface at a pixel dimension of ~250 m. As part of this mapping, targeted observations of selected areas are made using the MDIS, with pixel dimensions of ~10 m for monochrome imaging and 80 m for multispectral images. Resolution is greatest—more than a factor of 10 better than with standard mapping—for areas northward of 20° N, where the spacecraft

orbit is closest to Mercury. Several of the targeted areas (Figs. 1, A and B) show depressions, or hollows, that are irregular in shape with generally rounded edges. Horizontal dimensions range from tens of meters to several kilometers. The hollows are shallow and rimless, and many have high-reflectance interiors and diffuse bright halos. The interiors are mostly smooth and flat, but some have small bumps, hills, or mesas, the tops of which may be remnants of the original surface. Many form clusters, although some are isolated. The hollows appear fresh and lack superposed impact craters, implying that they are relatively young.

To date, we have found hollows within impact craters that span a range of sizes. The examples in Fig. 1, A and B, are on impact crater central peaks or the peak rings of impact basins. Additional examples on basin peak rings are shown in Fig. 1, C and D. Similar high-reflectance hollows occur on the floors, walls, and rims of some medium-sized impact craters (Fig. 1, E and F). The hollows are found in comparatively fresh (Kuiperian) rayed craters, more degraded craters, and basins in a variety of states of erosion.

Craters such as Tyagaraja and Sander (Fig. 2, A and B) exhibit extensive fields of coalescing bright-interior/bright-halo hollows on their floors, lending an etched appearance to the terrain. The etched terrain on Tyagaraja's floor displays some of the highest reflectance on the planet (~2.5 times the global average), has a relatively shallow ("blue") spectral slope (*2*), and lacks clear spectral features in MDIS multispectral data. Surfaces

with spectral properties such as those of the hollows in Figs. 1D and 2A were also seen in lower-spatial-resolution multispectral images from the Mariner 10 and MESSENGER flybys (*3–7*).

Materials with high reflectance and extremely blue color are global spectral outliers and have been termed "bright crater-floor deposits" (BCFDs) (*5–7*). MESSENGER flyby images indicated that BCFDs occur in several morphologic types, including varieties that have lobate outlines and those on central peaks and peak rings. Apart from Raditladi, Tyagaraja, and Sander (Figs. 1C and 2, A and B), prominent named examples include the deposits on the floors of the craters Balzac, de Graft, Kertesz, and Zeami and on the central peaks or peak rings of Eminescu and Vivaldi.

MESSENGER's orbital high-resolution and color imaging reveals that the areas identified as BCFDs are composed of hollows and etched terrain; hence, hollows are widespread across the planet (Fig. 3). Hollows have been found between ~66° N and 54° S and across all longitudes covered so far by orbital imaging. Many hollows occur in areas where there are exposures of low-reflectance material (LRM) (*5, 6*), a major global color-compositional unit thought to have been originally emplaced at depth (*8*).

Volcanism, explosive outgassing, collapse into a subsurface void, and loss of volatile-rich material through sublimation are capable of creating irregularly shaped depressions on planetary surfaces. Volcanism was an important and widespread process on Mercury (*9–14*). Extrusive and explosive volcanism can produce rimless depressions in the form of calderas, vents, and collapse pits. A number of probable pyroclastic vents and deposits have been identified on Mercury (*12, 13, 15–17*). Also, an intrusive magmatic process has been proposed as the source for a class of pit craters on Mercury (*18*), via collapse after withdrawal of magma from a near-surface chamber. However, the size and morphology of the pyroclastic vents and pit craters identified to date on Mercury differ from those of the hollows. Most of the irregular depressions associated with pyroclastic deposits are large [several tens of kilometers (*16, 17*)] relative to the hollows and typically occur as isolated depressions rather than in clusters. Moreover, the hollows occur on the tops and sides of central peak mountains as well as across impact crater walls and rims, which are unlikely locations for volcanic eruptions. The recognized pyroclastic deposits are associated with strong positive ("red") spectral slope across the visible and near-infrared (*5, 6, 15–17*) in contrast to the "blue" character of the hollows. Thus, if the

¹The Johns Hopkins University Applied Physics Laboratory, Laurel, MD 20723, USA. ²Department of Geological Sciences, Brown University, Providence, RI 02912, USA. ³Department of Terrestrial Magnetism, Carnegie Institution of Washington, Washington, DC 20015, USA. ⁴Smithsonian Institution, Washington, DC 20013, USA. ⁵Lunar and Planetary Laboratory, University of Arizona, Tucson, AZ 85721, USA. ⁶Faculty of Earth Sciences, China University of Geosciences, Wuhan, Hubei, 430074, P. R. China. ⁷School of Earth and Space Exploration, Arizona State University, Tempe, AZ 85251, USA. ⁸Institute of Planetary Research, German Aerospace Center, D-12489 Berlin, Germany.

*To whom correspondence should be addressed. E-mail: david.blewett@jhuapl.edu